chemistry proceedings

MDPI

Proceeding Paper

Investigating the Photophysical Properties and Biological Efficacy of BODIPY Derivatives as Photosensitizers in Photodynamic Therapy †

Raquel C. R. Gonçalves [1,2], Sónia C. S. Pinto [1], João Pina [3], Lígia C. Gomes-da-Silva [3], Susana P. G. Costa [1] and M. Manuela M. Raposo [1,*]

[1] Centre of Chemistry, University of Minho, Campus of Gualtar, 4710-057 Braga, Portugal; email1@email.com (R.C.R.G.); email2@email.com (S.C.S.P.); email3@email.com (S.P.G.C.)
[2] Advanced (Magnetic) Theranostic Nanostructures Lab, International Iberian Nanotechnology Laboratory, Av. Mestre José Veiga s/n, 4715-330 Braga, Portugal
[3] Department of Chemistry, Coimbra Chemistry Centre, University of Coimbra, Rua Larga, 3004-535 Coimbra, Portugal; email4@email.com (J.P.); email5@email.com (L.C.G.-d.-S.)
* Correspondence: mfox@quimica.uminho.pt
† Presented at the 27th International Electronic Conference on Synthetic Organic Chemistry (ECSOC-27), 15–30 November 2023; Available online: https://ecsoc-27.sciforum.net/.

Abstract: The selectivity of photosensitizers for light activation is a key advantage in photodynamic therapy (PDT), allowing for precise targeting while sparing healthy cells. BODIPY derivatives have emerged as promising PDT candidates due to their tunable photophysical properties and versatile synthesis. Herein, we explore the photophysical characterization and the in vitro photodynamic activity of BODIPY analogues *meso*-substituted with an anthracene moiety and functionalized with iodine atoms or formyl group at 2,6-position. The formylated anthracene-BODIPY derivative exhibited the highest tumor suppression under irradiation, making it a potential candidate as PDT photosensitizer.

Keywords: BODIPY derivative; cancer therapy; photosensitizers; PDT; singlet oxygen quantum yield

Citation: Gonçalves, R.C.R.; Pinto, S.C.S.; Pina, J.; Gomes-da-Silva, L.C.; Costa, S.P.G.; Raposo, M.M.M. Investigating the Photophysical Properties and Biological Efficacy of BODIPY Derivatives as Photosensitizers in Photodynamic Therapy. *Chem. Proc.* **2023**, *14*, x. https://doi.org/10.3390/xxxxx

Academic Editor(s):

Published: 15 November 2023

1. Introduction

Photosensitizers are light-activated compounds that play a crucial role in the field of photodynamic therapy (PDT), an emerging non-invasive therapeutic modality for the treatment of various diseases, including cancer. Photodynamic therapy combines light and photosensitizers in the presence of oxygen to generate cytotoxic reactive oxygen species and induce cellular death. In fact, PDT relies on the ability of photosensitizers to be selectively activated by light, allowing a precise local treatment, while minimizing collateral damage to healthy cells and tissues [1]. Moreover, studies have demonstrated that photodynamic therapy is able to trigger the immune system and enhance the anti-tumor immunity [2–4].

Amongst the well-known photosensitizers (e.g., porphyrins, chlorin, xanthene, and ruthenium-based complexes), BODIPY derivatives have shown promising potential because of their highly tunable photophysical properties and versatile synthetic accessibility. Several studies have explored the optimization of the BODIPY core to improve singlet-to-triplet intersystem crossing and efficiency to generate singlet oxygen (singlet oxygen quantum yields) [5–7]. For example, the halogen substitution at the BODIPY core significantly impacts their photophysical properties by reducing their fluorescence quantum yields while enhancing intersystem crossing to the triplet state, and consequently promoting the generation of singlet oxygen [8]. Similarly, complexing BODIPYs

with metals such as Ir(III) can transform a photoinactive dye into an efficient triplet sensitizer, suggesting these derivatives may act as effective PDT photosensitizers [9,10]. Moreover, the potential of BODIPY derivatives as singlet oxygen sensitizers extends beyond cancer treatment to the photodynamic inactivation of microbes, fungi, and viruses [11].

As an extension of the work developed in our research group [12,13], we report the design and evaluation of BODIPY derivatives functionalized with an anthracene moiety at *meso* and an iodine or formyl group at 2,6-positions of the core. The photophysical characterization of the derivatives and the in vitro PDT studies in cancer cells (4T1 cell line) were performed to determine their potential as PDT photosensitizers.

2. Methods and Materials

NMR spectrum was obtained on a Bruker Avance III 400 at an operating frequency of 400 MHz for ^{1}H, using the solvent peak as internal reference. The solvents are indicated in parenthesis before the chemical shift values (δ relative to TMS). Mass spectrometry analysis was performed at the "C.A.C.T.I. -Unidad de Espectrometria de Masas" at the University of Vigo, Spain. All reagents were purchased from Sigma-Aldrich, Acros and Fluka and used as received. TLC analysis was carried out on 0.25 mm thick precoated silica plates (Merck Fertigplatten Kieselgel 60F254) and the spots were visualized under UV light. Chromatography on silica gel was carried out on Merck Kieselgel (230–400 mesh). The synthesis of BODIPY derivatives **1**, **3** and **4** has been already published by our research group [13].

2.1. Synthesis of BODIPY Derivative 2

N-iodosuccinimide (NIS, 0.57 mmol) was dissolved in dichloromethane (DCM, 6 mL) and added to a solution of BODIPY **1** (0.12 mmol) in DCM (6 mL). The reaction was stirred for 2 h at room temperature. The solvent was evaporated under low-pressure conditions. The crude product was resuspended in ethyl ether (15 mL) and the solid was filtered under vacuum (0.042 g, η = 57%), giving the pure compound **2** (Figure 1), as a red solid.

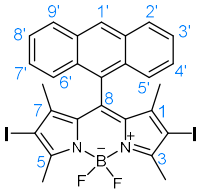

Figure 1. Structure of BODIPY derivative **2**.

^{1}H NMR (400 MHz, $CDCl_3$): δ = 0.68 (s, 6H, CH_3-1 and CH_3-7), 2.72 (s, 6H, CH_3-3 and CH_3-5), 7.45 (dt, J = 1.2 and 8 Hz, 2H, H-3′ and H-8′), 7.52 (dt, J = 1.2 and 8 Hz, 2H, H-4′ and H-7′), 7.83 (dd, J = 0.8 and 8 Hz, 2H, H-2′ and H-9′), 8.07 (d, J = 8.4 Hz, 2H, H-5′ and H-6′), 8.64 (s, 1H, H-1′) ppm.

MS (ESI) m/z (%): 678 ($[M + 2]^{+\bullet}$, 8), 677 ($[M + 1]^{+\bullet}$, 28), 676 ($[M]^{+\bullet}$, 7), 550 (100), 469 (50), 453 (46), 447 (80), 381 (35), 381 (35), 359 (38), 227 (33), 226 (30), 149 (45); HRMS (ESI) m/z: $[M + 1]^{+\bullet}$ calcd for $C_{27}H_{22}BF_2I_2N_2$, 676.9928; found 676.9910.

2.2. Photophysical Characterization

The photophysical characterization of BODIPY derivatives was performed in tetrahydrofuran (THF) and toluene solutions. The photophysical characterization of the BODPY **2** was evaluated as previously reported by our group for BODIPY derivatives **1**, **3** and **4** [13].

2.3. Cell Culture and In Vitro Assays

Murine mammary carcinoma cell line from a BALB/cfC3H mouse (4T1 cells) were grown in Dulbecco's modified Eagle's medium (DMEM) supplemented with 10% fetal bovine serum (FBS) and 1% of penicillin-streptomycin. Cells were maintained at 37 °C in a humidified incubator with a 5% CO_2 atmosphere. Cells were plated and passaged according to ATCC recommendations and were used for the experiments while in the exponential growth phase.

The stock solutions of the BODIPY derivatives 1, 2 and 3 were prepared in DMSO (10 mM) and the final DMSO percentage in each well was adjusted to be less than 1%.

2.3.1. Cellular Uptake Assay

4T1 Cells (40,000 cells/well) were seeded in 24-well plates in a final volume of 1 mL of DMEM and incubated for 24 h at 37 °C in a humidified incubator with 5% CO_2. Then, cells were incubated with the BODIPY derivatives at a concentration of 2.5 μM. After different incubation times (0.5, 1, 3, 6 and 24 h), the cells were washed and detached with 250 μL of trypsin, transferred to a 96-well U-shaped plate, and centrifuged at 1200 rpm for 5 min. The pellet was resuspended in 200 μL PBS. And the cells were analyzed by flow cytometry using the Novocyte 3000 cytometer (ACEA) with 488 nm laser excitation and filter 530/30. Data is presented as mean fluorescence intensity (MFI) normalized to the mean fluorescence of untreated cells. This experiment was performed in duplicate and repeated in two sets of tests. Statistical analysis of results was performed using GraphPad Prism 5.0 software. One-way ANOVA was conducted to study the statistical significance of the incubation times related to 6 h of incubation and significance levels were established at $p < 0.05$.

2.3.2. Dark Toxicity and Phototoxicity of the BODIPY Derivatives

4T1 Cells (6000 cells/well) were plated in 96-well plates and kept in incubation for 24 h to allow the attachment of the cells. Cells were then treated with compounds in a concentration range from 0 to 100 μM. After 24 h, cell viability (dark toxicity) was determined by the Resazurin assay. Phototoxicity was evaluated in parallel experiments using two sets of light doses (0.6 $J.cm^{-2}$ and 2 $J.cm^{-2}$) and two sets of incubation times (30 min and 6 h). Cells were treated with the BODIPY derivatives in a concentration range from 0.16 to 5 μM and after each incubation time, cells were washed with PBS and 200 μL of RPMI without Phenol Red was added. Controls of the untreated cell were included on every plate. The cells were then irradiated with a green LED light source (505 nm). A correction factor from the overlap of the absorption spectra between the laser and each compound was calculated and applied to achieve accurate light dose [14]. After irradiation, cells were washed and fresh DMEM was added. The cell viability was determined by the Resazurin assay after 24 h post-illumination treatment. Both studies were performed in triplicates and repeated in two sets of tests. Statistical analysis of results was performed using GraphPad Prism 5.0 software.

3. Results and Discussion

3.1. Synthesis and Photophysical Characterization of the BODIPY Derivatives

In Scheme 1 is represented the synthetic route to obtain the derivatives bearing an anthracene group at meso position and different functionalization at position 2 and/or 6 of the BODIPY core. The synthesis of BODIPY derivatives **1**, **3** and **4** has been recently reported by our research group [13]. We employed the well-known Lindsey's method (BODIPY precursor **1**), followed by the halogenation reaction using N-iodosuccinimide (NIS) to obtain the BODIPY derivative **2** functionalized with iodine at positions 2 and 6.

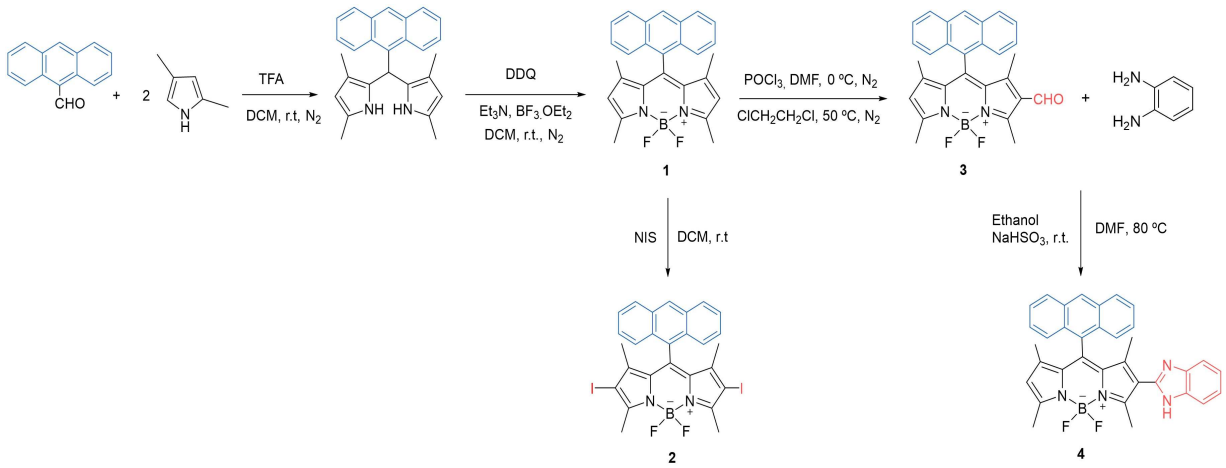

Scheme 1. Synthesis of the BODIPY derivatives **1**-**4**.

3.2. Photophysical Characterization

A comprehensive photophysical evaluation of the BODIPY derivatives was performed to investigate the effects of the substituent groups on the photophysical properties, including the singlet oxygen generation efficiency (Table 1). The heavy atom effect of the iodine atoms in BODIPY **2** and the electron-withdrawing behavior of the formyl group in BODIPY **3** promoted a significant reduction in the fluorescence quantum yield and concomitant increase in the triplet formation quantum yield (estimated from the efficient singlet-oxygen sensitization quantum yield), when compared to the BODIPY precursor **1.** However, it was observed that the introduction of the benzimidazole heterocycle (BODIPY **4**) significantly decreased the singlet oxygen sensitization quantum yield value (ϕ_Δ = 0.04 vs. 0.27, 0.76 and 0.74 for compounds **1**, **2** and **3** in tetrahydrofuran solution, respectively), which may ultimately impair the compound's in vitro photosensitization efficacy.

Table 1. Photophysical data (including absorption, λ_{abs}, and fluorescence emission maxima, λ_{fluo}, fluorescence quantum yields, ϕ_F, and singlet oxygen sensitization quantum yields, ϕ_Δ) for BODIPY derivatives **1**–**4**, in toluene (a) and tetrahydrofuran solution (b) at 293 K.

Compound	λ_{abs} (nm)	λ_{fluo} (nm)	ϕ_F	ϕ_Δ
1	508 [a]	520 [a]	0.82 [a]	0.04 [a]
	505 [b]	515 [b]	0.43 [b]	0.27 [b]
2	542 [a]	559 [a,b]	0.02 [a]	0.93 [a]
	540 [b]		0.003 [b]	0.76 [b]
3	507 [a]	522 [a]	0.08 [a]	0.75 [a]
	502 [b]	525 [b]	0.02 [b]	0.74
4	521 [a,b]	579 [a]	0.52 [a]	nd [a]
		585 [b]	0.35 [b]	0.04 [b]
		585 [b]		

3.3. In Vitro Assays

Considering the photophysical data obtained regarding the singlet oxygen quantum yields (ϕ_Δ), the in vitro phototoxicity of the BODIPY derivatives **1**, **2** and **3** were investigated in 4T1 cells.

Initially, the cellular uptake was investigated through flow cytometry as depicted in Figure 2, which demonstrated that compounds **1** and **3** are rapidly internalized by the cells, reaching a maximum at 6 h of incubation. In contrast, the fluorescence detected in the cells treated with BODIPY **2** was significantly lower. The differences in the level of

cellular uptake between the three compounds might be due to their different ϕ_F, but also due the lower solubility of compound **2** in aqueous medium, which could affect the capability to diffuse through the cell membrane.

The cell viability was evaluated in the dark, after 24 h of incubation with the compounds and no cytotoxicity was observed, even at the highest concentration tested (Figure 3a). In contrast, irradiation with a light dose of 0.6 J.cm^{-2} after 30 min of incubation with the compound **2** resulted in cell death with concentrations above 2.5 μM (IC_{50} = 2.92 μM), whilst compounds **1** and **3** did not affect cell viability, even at the highest concentration tested (Figure 3b). The experiment was repeated, yet with an incubation time of 6 h, however the results did not significantly differ from the previous study (Figure 3c). Therefore, since a higher incubation time did not increase the BODIPYs' phototoxicity, a light dose of 2 J.cm^{-2} was applied. Under this condition, it was observed that not only BODIPY **1** became more toxic at lower concentrations (IC_{50} = 0.88 μM) but also compound **1** was capable of considerably decreasing cell viability (IC_{50} = 2.05 μM) (Figure 3d). Unexpectedly, the phototoxic effect of the BODIPY derivative **3** was not observed, although the compound displayed the highest singlet oxygen quantum yield. This could be attributed to its low solubility in aqueous medium.

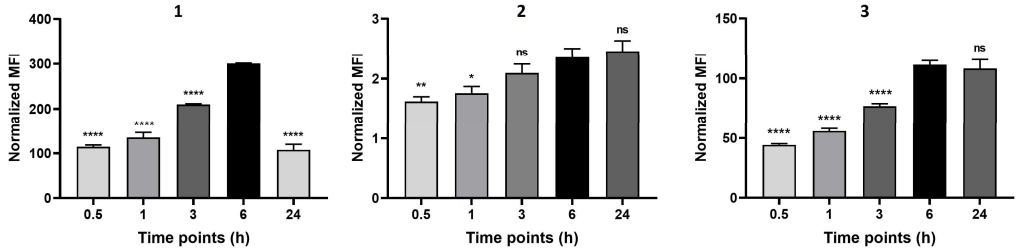

Figure 2. Cellular uptake of the BODIPY derivatives **1**, **2** and **3** in 4T1 cells. Cell uptake was monitored by flow cytometry after 0.5, 1, 3, 6 and 24 h of incubation with 2.5 μM of the compounds. Data is presented as mean ± SEM (n = 2).

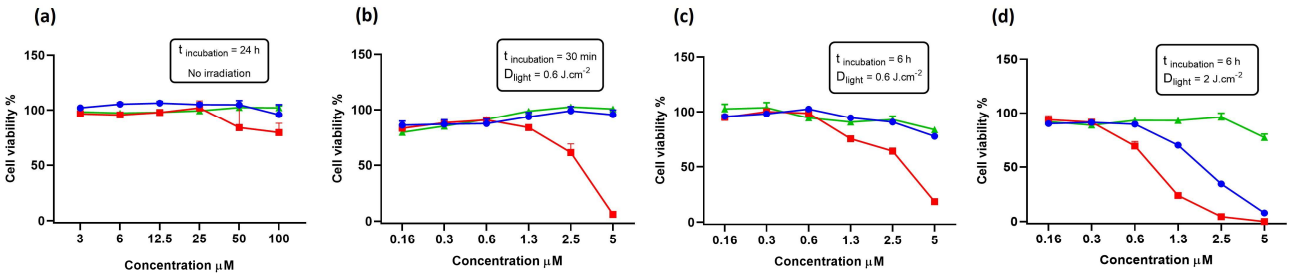

Figure 3. Cell viability of 4T1 cells incubated with BODIPY derivatives **1** (blue), **2** (green) and **3** (red) for 24 h without irradiation (**a**); for 30 min and irradiated with 0.6 J.cm^{-2} (**b**); for 6 h and irradiated with 0.6 J.cm^{-2} (**c**) and for 6h and irradiated with 2 J.cm^{-2} (**d**).

4. Conclusions

In conclusion, here we reported a series of BODIPY derivatives bearing an anthracene moiety at *meso* position and functionalized at position 2 and/or 6 with a formyl group or iodine atoms. The photophysical evaluation in toluene and THF solutions revealed that the derivatives substituted with the halogen atoms (BODIPY **2**) and the electron-withdrawing formyl group (BODIPY **3**) displayed the greatest singlet oxygen quantum yields. The in vitro assays demonstrated that BODIPY precursor **1** and BODIPY **3** were easily internalized, and the three compounds were non-toxic for 4T1 cancer cells in the dark. However, under irradiation with a light dose of 2 J.cm^{-2}, compound **1** and **3** reduced cell viability for 50% with only 2.05 and 0.88 μM, respectively. These results sug-

gest the promising potential, specially the formylated BODIPY derivative, as photosensitizer in photodynamic therapy.

Author Contributions: Conceptualization, M.M.M.R., J.P. and L.C.G.-d.-S.; methodology, R.C.R.G., M.M.M.R., J.P., L.C.G.-d.-S. and S.P.G.C.; validation, M.M.M.R., J.P., L.C.G.-d.-S. and S.P.G.C.; formal analysis, R.C.R.G., M.M.M.R., J.P., L.C.G.-d.-S. and S.P.G.C.; investigation, R.C.R.G. and S.C.S.P.; resources, M.M.M.R., J.P., L.C.G.-d.-S. and S.P.G.C.; writing—original draft preparation, R.C.R.G. and S.C.S.P.; writing—review and editing, R.C.R.G., M.M.M.R., J.P., L.C.G.-d.-S. and S.P.G.C.; supervision, M.M.M.R., J.P., L.C.G.-d.-S. and S.P.G.C.; project administration, M.M.M.R., J.P., L.C.G.-d.-S. and S.P.G.C.; funding acquisition, M.M.M.R., J.P., L.C.G.-d.-S. and S.P.G.C.; All authors have read and agreed to the published version of the manuscript.

Funding: This research was funded by Fundação para a Ciência e Tecnologia (FCT) and FEDER (European Fund for Regional Development)-COMPETE-QRENEU through the Chemistry Research Centre of the University of Minho (ref. CQ/UM (UID/QUI/00686/2020)), and the Coimbra Chemistry Centre (refs. UIDB/00313/2020 and UIDP/00313/2020), project PTDC/QUI-OUT/3143/2021 and a PhD grant of R.C.R. Gonçalves (SFRH/BD/05278/2020). The NMR spectrometer Bruker Avance III 400 is part of the National NMR Network and was purchased within the framework of the National Program for Scientific Re-equipment, contract REDE/1517/RMN/2005 with funds from POCI 2010 (FEDER) and FCT.

Institutional Review Board Statement: Not applicable.

Informed Consent Statement: Not applicable.

Data Availability Statement: Not applicable.

Conflicts of Interest: The authors declare no conflict of interest.

References

1. Lan, M.; Zhao, S.; Liu, W.; Lee, C.; Zhang, W.; Wang, P. Photosensitizers for Photodynamic Therapy. *Adv. Healthc. Mater.* **2019**, *8*, 1900132. https://doi.org/10.1002/adhm.201900132.
2. Sasaki, M.; Tanaka, M.; Kojima, Y.; Nishie, H.; Shimura, T.; Kubota, E.; Kataoka, H. Anti-Tumor Immunity Enhancement by Photodynamic Therapy with Talaporfin Sodium and Anti-Programmed Death 1 Antibody. *Mol. Ther. Oncolytics* **2023**, *28*, 118–131. https://doi.org/10.1016/j.omto.2022.12.009.
3. Reginato, E. Immune Response after Photodynamic Therapy Increases Anti-Cancer and Anti-Bacterial Effects. *World J. Immunol.* **2014**, *4*, 1. https://doi.org/10.5411/wji.v4.i1.1.
4. S. Lobo, A.C.; Gomes-da-Silva, L.C.; Rodrigues-Santos, P.; Cabrita, A.; Santos-Rosa, M.; Arnaut, L.G. Immune Responses after Vascular Photodynamic Therapy with Redaporfin. *J. Clin. Med.* **2019**, *9*, 104. https://doi.org/10.3390/jcm9010104.
5. Prieto-Montero, R.; Prieto-Castañeda, A.; Sola-Llano, R.; Agarrabeitia, A.R.; García-Fresnadillo, D.; López-Arbeloa, I.; Villanueva, A.; Ortiz, M.J.; De La Moya, S.; Martínez-Martínez, V. Exploring BODIPY Derivatives as Singlet Oxygen Photosensitizers for PDT. *Photochem. Photobiol.* **2020**, *96*, 458–477. https://doi.org/10.1111/php.13232.
6. Malacarne, M.C.; Gariboldi, M.B.; Caruso, E. BODIPYs in PDT: A Journey through the Most Interesting Molecules Produced in the Last 10 Years. *Int. J. Mol. Sci.* **2022**, *23*, 10198. https://doi.org/10.3390/ijms231710198.
7. Wang, J.; Gong, Q.; Wang, L.; Hao, E.; Jiao, L. The Main Strategies for Tuning BODIPY Fluorophores into Photosensitizers. *J. Porphyr. Phthalocyanines* **2020**, *24*, 603–635. https://doi.org/10.1142/S1088424619300234.
8. Gorbe, M.; Costero, A.M.; Sancenón, F.; Martínez-Máñez, R.; Ballesteros-Cillero, R.; Ochando, L.E.; Chulvi, K.; Gotor, R.; Gil, S. Halogen-Containing BODIPY Derivatives for Photodynamic Therapy. *Dyes Pigm.* **2019**, *160*, 198–207. https://doi.org/10.1016/j.dyepig.2018.08.007.
9. Tabrizi, L.; Chiniforoshan, H. New Cyclometalated Ir (III) Complexes with NCN Pincer and Meso-Phenylcyanamide BODIPY Ligands as Efficient Photodynamic Therapy Agents. *RSC Adv.* **2017**, *7*, 34160–34169. https://doi.org/10.1039/C7RA05579J.
10. Palao, E.; Sola-Llano, R.; Tabero, A.; Manzano, H.; Agarrabeitia, A.R.; Villanueva, A.; López-Arbeloa, I.; Martínez-Martínez, V.; Ortiz, M.J. AcetylacetonateBODIPY-Biscyclometalated Iridium(III) Complexes: Effective Strategy towards Smarter Fluorescent Photosensitizer Agents. *Chem. Eur. J.* **2017**, *23*, 10139–10147. https://doi.org/10.1002/chem.201701347.
11. Carpenter, B.; Situ, X.; Scholle, F.; Bartelmess, J.; Weare, W.; Ghiladi, R. Antiviral, Antifungal and Antibacterial Activities of a BODIPY-Based Photosensitizer. *Molecules* **2015**, *20*, 10604–10621. https://doi.org/10.3390/molecules200610604.
12. Gonçalves, R.C.R.; Pina, J.; Costa, S.P.G.; Raposo, M.M.M. Synthesis and Characterization of Aryl-Substituted BODIPY Dyes Displaying Distinct Solvatochromic Singlet Oxygen Photosensitization Efficiencies. *Dyes Pigm.* **2021**, *196*, 109784. https://doi.org/10.1016/j.dyepig.2021.109784.
13. Gonçalves, R.C.R.; Belmonte-Reche, E.; Pina, J.; Costa Da Silva, M.; Pinto, S.C.S.; Gallo, J.; Costa, S.P.G.; Raposo, M.M.M. Bioimaging of Lysosomes with a BODIPY pH-Dependent Fluorescent Probe. *Molecules* **2022**, *27*, 8065. https://doi.org/10.3390/molecules27228065.

14. Schaberle, F.A. Assessment of the Actual Light Dose in Photodynamic Therapy. *Photodiagnosis Photodyn Ther.* **2018**, *23*, 75–77. https://doi.org/10.1016/j.pdpdt.2018.06.009.